Assessing Agricultural Water Productivity in Desert Farming System of Saudi Arabia

Virupakshagowda C. Patil, Khalid A. Al-Gaadi, Rangaswamy Madugundu, ElKamil H. M. Tola, Samy Marey, Ali Aldosari, Chandrashekhar M. Biradar, and Prasanna H. Gowda

Abstract—The primary objective of this study was to assess the water productivity (WP) of the annual (wheat, barley, and corn) and biennial (alfalfa and Rhodes grass) crops cultivated under center-pivot irrigation located over desert areas of the Al-Kharj region in Saudi Arabia. The Surface Energy Balance Algorithm for Land (SEBAL) was applied to Advanced Spaceborne Thermal Emission and Reflection Radiometer (ASTER) images to obtain evapotranspiration (ET) for assessing WP and irrigation performance (IP) of crops. Crop productivity (CP) was estimated using Normalized Difference Vegetation Index (NDVI) crop productivity models. The predicted CP (CP_P) for corn varied from 12 690 to 14 060 kg/ha and from 6000 to 7370 kg/ha for wheat. The CP_P for alfalfa and Rhodes grass was 42 450 and 58 210 (kg/ha/year), respectively. The highest predicted WP was observed in wheat ($0.80-2.01$ kg/m^3) and the lowest was in alfalfa ($0.38-0.46$ kg/m^3). The deviation between SEBAL predicted ET (ET_P) and weather station recorded ET (ET_W) was 10%. The performance of the prediction models was assessed against the measured data. The overall mean bias/error of the predictions of CP, ET, and WP was 9.4%, -2.68%, and 9.65%, respectively; the root mean square error (RMSE) was 1996 (kg/ha), 2107 (m^3/ha), and 0.09 (kg/m^3) for CP, ET, and WP, respectively. When CP was converted into variations between the actual and predicted, the variations were 8% to 12% for wheat, 14% to 20% for corn, 17% to 35% for alfalfa, 3% to 38% for Rhodes grass, and 4% for barley.

Index Terms—ASTER image, center-pivot irrigation system, crop productivity, evapotranspiration, water use.

I. INTRODUCTION

AGRICULTURE is the largest consumer of freshwater in the world [1]. In arid and semiarid environments,

V. C. Patil, K. A. Al-Gaadi, R. Madugundu, and E. H. M. Tola are with the Precision Agriculture Research Chair, Department of Agricultural Engineering, College of Food and Agriculture Sciences, King Saud University, Riyadh 11451, Saudi Arabia (e-mail: vpatil@ksu.edu.sa; kgaadi@ksu.edu.sa; rmadugundu@ksu.edu.sa; etola@ksu.edu.sa).

S. Marey was with Precision Agriculture Research Chair, Department of Agricultural Engineering, College of Food and Agriculture Sciences, King Saud University, Riyadh 11451, Saudi Arabia. He is now with the National Plan for Science and Technology, King Saud University, Riyadh 11451, Saudi Arabia (e-mail: smarey@ksu.edu.sa).

A. Aldosari is with the Department of Geography, College of Arts, King Saud University, Riyadh 11451, Saudi Arabia (e-mail: adosari@ksu.edu.sa).

C. M. Biradar is with the International Center for Agricultural Research in Dry Areas (ICARDA), Amman, Jordan (e-mail: c.biradar@cgair.org).

P. H. Gowda is with the USDA-ARS, Conservation and Production Research Lab, Bushland, TX 79012 USA (e-mail: Prasanna.Gowda@ars.usda.gov).

Color versions of one or more of the figures in this paper are available online at http://ieeexplore.ieee.org.

Digital Object Identifier 10.1109/JSTARS.2014.2320592

competition for freshwater has been steadily increasing among agricultural, domestic, and industrial sectors [2]. This competition will further increase with ever growing concerns of climate change and its variability, population growth, economic development, and environmental impacts. The demand for water in the Middle East and North African (MENA) region that was 270 km^3/year in 2000 is expected to increase to 393 km^3/year [3] or 460 km^3/year [4] in 2050.

The rapid dwindling of finite water resources and the steady increase in demand for food are the major obstacles for attaining agricultural sustainability in Saudi Arabia. Agriculture in general and irrigation in particular consume over 80% of the freshwater used in Saudi Arabia. In 2012, freshwater consumption for the agricultural sector in Saudi Arabia was estimated at 86%—an increase of 6% between 2008 and 2012 [5]. Water used for irrigation is pumped from deep aquifers (up to 1000 m) to feed center-pivot irrigation systems at enormous economic and environmental costs. This situation creates an urgent need for attaining agricultural sustainability, but it is extremely difficult to maintain equilibrium between water and food securities. This critical equilibrium emphasizes the Kingdom's need for strategic technologies and methods to drastically reduce the current depletion rate of groundwater resources and optimize water consumption without reducing agricultural production. This can only be achieved through the efficient use of irrigation water. Therefore, increasing water productivity (WP) in the agricultural sector is crucial for water conservation efforts that can serve other competitive and critical needs such as domestic, industrial, environmental, and recreational purposes.

WP is determined from biological/economic yield of crops and the quantity of water used to produce that yield. It is one of the key indicators for evaluating the efficiency of water use in agriculture. Any attempt to improve water use efficiency in irrigated agriculture must be based on reliable estimates of seasonal/total evapotranspiration (ET), which has a major impact on water management. ET varies regionally and seasonally according to weather conditions [6]. Understanding the variations in ET is essential for the management of water resources, particularly in hyper-arid regions of Saudi Arabia, where crop water demand exceeds precipitation by several folds and requires irrigation from groundwater resources to meet the deficit. ET values are not only useful for developing WP maps at field and regional scales, but are also useful for precision irrigation purposes.

Satellite-based remote sensing is a robust, economic, and efficient tool for estimating ET, WP, and the assessment of irrigation performance (IP). Monitoring the temporal changes of the key parameters used in these estimates through employing
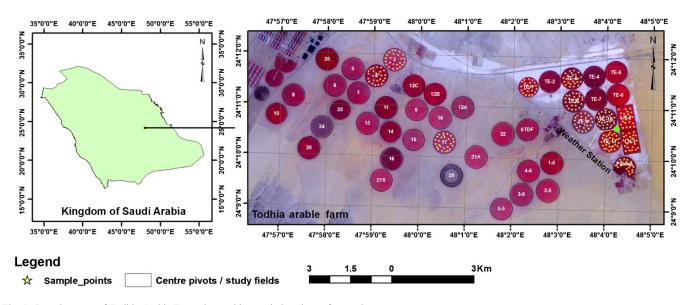
Fig. 1. Location map of Todhia Arable Farm along with sample locations of ground measurements.

remote sensing techniques can significantly contribute to irrigation management [7], [8]. A remote sensing approach overcomes constraints such as data scarcity and scale limitations and reduces uncertainties by covering large spatial domains over time.

Various surface energy balance models such as Surface Energy Balance Algorithm for Land (SEBAL) [9], Simplified Surface Energy Balance Index (S-SEBI) [10], Simplified Surface Energy Balance (SSEB) [11], and Mapping Evapotranspiration with Internalized Calibration (METRIC) [12] have been widely used around the globe for computing ET. The SEBAL model has been predominantly used to estimate ET [9], [13], WP, and IP [14]–[16]. SEBAL was applied to NOAA-AVHRR images to compute the accumulated groundwater abstraction for a 30-year period (1975–2004) in Saudi Arabia, and it was found to be 833 mm per year on average [17]. In another study, census data and crop water requirement models were used for estimating a nationwide abstraction of ground water in Saudi Arabia, which was reported to be 23 $km^3/$ per year for 2010 [18].

In view of the very low WP of the majority of crops grown under center-pivot irrigation systems in Saudi Arabia, there are ample opportunities for significant improvement. One of these opportunities was highlighted in a research study conducted to explore the potential of adopting proper cropping pattern based on water demand [19]. The results of that study showed great potential for enhancing food and water security in Saudi Arabia through producing alternate crops in regions where WP is high. In view of the pressing need to assess the WP of agricultural fields irrigated through center-pivot irrigation systems, this study was undertaken with the goal of developing a WPM using Advanced Space borne Thermal Emission and Reflection Radiometer (ASTER) satellite imagery for alfalfa, Rhodes grass, corn, wheat, and barley crops across spatial–temporal domains. The outcome of the study will be helpful in determining both the spatial and temporal variability in WP and in selecting the right crop at the right cultivating season for the optimal use of groundwater resources.

II. MATERIALS AND METHODS

A. Study Area

The study was carried out on the Todhia Arable Farm (TAF), a commercial farm with 47 fields utilizing center-pivot irrigation systems spread across an area of 6967 ha. The farm lies within the latitudes of $24°10'22.77''$ and $24°12'37.25''$N and within the longitudes of $47°56'14.60''$E and $48°05'08.56''$E (Fig. 1). Wheat, alfalfa, Rhodes grass, corn, and barley are cultivated to meet the fodder demand of cattle farms. Table I shows the cropping patterns and acreage of the study area. The crop acreage under alfalfa and corn was 580 and 227 ha, respectively, in 2012, and increasing to 900 and 640 ha, respectively, in 2013. The acreage under Rhodes grass and wheat crops decreased from 1430 and 437 ha, respectively, in 2012, to 542 and 100 ha, respectively, in 2013. However, barley was cultivated only in 2013. The season-wide cropping periods of all the investigated crops is provided in Table II.

B. Ground Truth Data Collection

The geo-referenced data of the ground-measured Normalized Difference Vegetation Index hereafter referred to as $NDVI_{(G)}$ and the ground-measured Leaf Area Index hereafter referred to as $LAI_{(G)}$ were collected synchronous to the dates of the satellite overpasses. The $NDVI_{(G)}$ and $LAI_{(G)}$ ground truth data collection schedules are presented in Table III.

Of the 47 pivots of the farm, 11 pivots (23%) were considered as samples for modeling. About 270 ground-based "point data" of the $NDVI_{(G)}$ and $LAI_{(G)}$ were collected from these 11 pivots; approximately, 25 random sample points from each pivot. Of the 270 ground points, 162 points (60%) were used for the development of NDVI crop productivity (CP) models and the remaining 108 (40%) were used for validation. The location of these sample points is depicted in Fig. 1.

The data on the quantity of water applied (WA) and the CP of the harvested crops for all the 47 pivots were obtained from the

TABLE I
CROPPING PATTERN IN TODHIA ARABLE FARM FOR THE YEAR 2012 AND 2013

Year	Crop	Total number of fields	Pivot (field) number	Total area (ha)
2012	Alfalfa	15	10, 25, 12B, 12 C, 1–5, LIN, TE1, TE10, TE2, TE3, TE4, TE5, TE6, TE7, TE8	580
	Corn	5	5, 7, 23, LIN, PAL	227
	Rhodes grass	29	2–8, 11, 13–18, 20, 22–24, 26, 12a, 21a, 21 s, 2–5, 3–5, 4–5, 5–5, 6TDF, TE11, TE9	1430
	Wheat	10	4, 11, 14, 18, 26, 3–5, LIN, PAL, TE11	437
2013	Alfalfa	18	2–8, 13, 14, 16, 20, 22–24, 26, 12a, 21a, 6TDF, TE11	900
	Barley	9	5, 11, 15, 17, 18, 21 s, 2–5, 4–5, TE9	450
	Corn	12	5, 1–5, LIN, TE1, TE10, TE2, TE3, TE4, TE5, TE6, TE7,TE8	640
	Rhodes grass	16	10, 11, 15, 17, 18, 25, 12B, 12 C, 21 s, 2–5, 3–5, 4–5, 5–5, PAL, TE12, TE9	542
	Wheat	2	3–5, TE10	100

TABLE II
SOWING DATES OF CROPS IN TODHIA ARABLE FARM, SAUDI ARABIA

Sl. No	Crops		Sowing period	
1	Cropping period		2011–2012	2012–2013
	Annual crops	Corn	Mar. 21, 2012 to Apr. 30, 2012; Aug. 18, 2012 to Sep. 4, 2012	Mar. 2–8, 2013
		Wheat	Nov. 26, 2011 to Jan. 1, 2012	Dec. 11, 2012
		Barley	Not applicable	Dec. 22–28, 2012
2	Cropping period		2010–2012	2012–2014
	Biennial crops	Alfalfa	Nov. 24, 2010 to Dec. 2, 2010	Nov. 18, 2012 to Dec. 6, 2012
		Rhodes grass	Apr. 1, 2011 to May 4, 2011; Mar. 25, 2012 to May 24, 2012	Mar. 4, 2013 to Apr. 12, 2013

TABLE III
SCHEDULE OF GROUND TRUTH DATA COLLECTION FOR THE YEAR 2012 AND 2013

Year	Crop	Data collection date	Pivot field no.
2012	Wheat	Feb. 04, Feb. 13, Feb. 17, Mar. 4, Mar. 20	TE-11
	Alfalfa	Mar. 20, Apr. 23, Jun. 1, Jun. 17, Jul. 3, Jul. 19, Aug. 4, Sep. 11, Oct. 7, Nov. 15	TE-1, TE-10, TE-8, LIN
	Corn	May 31, Jun. 16, Jul. 3, Jul. 18, Aug. 3	PAL, LIN
	Rhodes grass	24 Apr, Jun. 2, Jun. 18, Jul. 4, Jul. 18, Aug. 4, Sep. 12, Oct. 7, Nov. 15	P2, P4, TE-11, TE 9
2013	Wheat	Feb. 12, Mar. 16	TE-10
	Alfalfa	Feb. 12, Mar. 16	TE-11, P2, P4
	Corn	Mar. 16, May 19	TE-1, TE-3
	Rhodes grass	May 19	TE-9, P17
	Barley	Feb. 12, Mar. 16	TE-9, P17

TAF Manager. Of these, 11 pivots (23%) were used for modeling and the remaining 36 pivots were used for validation.

The $\mathrm{NDVI}_{(G)}$ was measured in the field on the dates of the satellite overpass by using the crop circle (Model ACS-470) of Holland Scientific, USA. The crop circle device was calibrated through configuration of a 670-nm filter in channel 1, an NIR filter in channel 2 and a 550-nm filter in channel 3 of the sensor socket for measuring $\mathrm{NDVI}_{(G)}$. Map mode
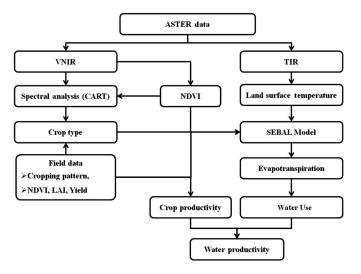
Fig. 2. Water productivity prediction flow chart.

measurements with 2 samples/s were used for field data collection. To determine the field data coordinates, an OmniSTAR GPS receiver (Model 9200-G2) was connected to the Crop Circle at a baud rate of 9600. Field data measurements were recorded with the Crop Circle positioned at 1 m above the crop canopy.

The $LAI_{(G)}$ was determined on the dates of the satellite overpass by using the plant canopy analyser (Model PCA-2200) of LiCOR Biosciences, USA. To compute a single LAI value at each location, one above canopy and five below canopy readings were recorded. The above and below canopy measurements were made by using a "fisheye" optical sensor with a 148° angle of view. Respective geo-locations were collected using a handheld Trimble GPS receiver (Model-Geo XH 600). An azimuth mask of a 180° view cap was used on a PCA-2200 sensor during data collection to obscure the bright sky and thus eliminate the shading effect of the instrument operator. The measured $NDVI_{(G)}$ and $LAI_{(G)}$ were used to correct the ASTER-derived NDVI and LAI and subsequently used in the selection of anchor pixels (cold and hot) for the SEBAL model.

Meteorological data were collected from an automatic weather station (Vintage Pro2 wireless station) installed at the farm. Meteorological data such as wind speed, humidity, hourly solar radiation, and air temperature were used for processing the net radiation (R_n), soil heat flux (G), and sensible heat flux (H) used for the SEBAL Model. The wind speed (u) at the time of the satellite overpass was used for the computation of sensible heat flux (H) and humidity; which were utilized for the estimation of reference ET (ET_r). Solar radiation data were used for the estimation of the image cloudiness and to adjust the atmospheric transmissivity (τ_{sw}). A data assimilation approach was used to compute WP. CP and ET data were used to compute the final WP map (Fig. 2).

C. Processing of ASTER Images

Time series of level 1B (ASTL 1 b) ASTER images (Appendix I) pertaining to Paths 164 and 165 procured from Japan Space Systems (Available: http://gds.ersdac.jspacesystems.or.jp) were used in this study to generate the ET, CP, and WP map of the

TAF. Of the 15 procured images, 12 were from 2012 and the remaining 3 were from 2013. These images covered the entire range of crop phenology for all crops. In the case of wheat, barley, and corn, the images covered the peak growth stage, whereas the images covered all the growth stages between two harvests/cuts for alfalfa and Rhodes grass. The details of the ASTER data, such as the date of acquisition, the sun elevation angle, the zenith angle, and the distance between sun and earth (which were used in radiometric calibration), are presented in Table IV.

The acquired images were georeferenced and radiometrically calibrated by adopting a radiative transfer model using precalibrated coefficients [20]. At sensor, temperatures (K) were obtained from thermal bands, as described by Ghulam [21]. The NDVI, which is widely used for the assessment of remotely sensed data, was derived from the visible and near-infrared bands [22].

D. Water Productivity Mapping

WP is defined as either the amount of yield produced per unit volume of water (kg of $yield/m^3$ of water) or as a monetary value of the yield produced per unit volume of water [23]. Water Productivity Mapping (WPM) was achieved in three steps: 1) Crop Productivity Mapping (CPM), 2) Water Use (ET) Mapping (WUM) and 3) Water Productivity Mapping (WPM) [23]. Field-measured crop productivity data were related to the NDVI to obtain CP models. The best fit CP models were extrapolated to larger areas by using remotely sensed data to obtain CPM. WUM was prepared by using crop ET. The ET_{24} (per day) was obtained from ASTER data by applying the SEBAL model [9]. WPM was generated for the entire TAF by dividing the CPM by the WUM.

1) Crop Productivity Mapping: CP is a very important end-of-season observation that integrates the cumulative effect of weather and management practices over the entire crop growth season. A remote sensing approach provides both CP assessments and possible variations across fields. Linear relationships between CP and the NDVI at the crop heading stage were observed [24]. In this study, a scatter plot for each crop was drawn between the corrected ASTER-derived NDVI (x-axis) and CP (y-axis) for the development of CP prediction models. The NDVI at the ear-head emergence stage in wheat and barley, the flag leaf stage in corn, and the flowering stage in alfalfa and Rhodes grass were considered for CP estimations.

The CP model was developed using (1)

$$Y = a*X \pm b \tag{1}$$

where Y is the predicted CP (kg/ha), X is the NDVI, and a and b are the constants.

Measured CP (CP_A) data were collected from the TAF records and correlated with the respective field's NDVI derived from ASTER images. Remote sensing-based CP (CP_P) of corn, barley, and wheat was computed by multiplying the above ground biomass (AGB) by the Harvest Index (HI), a function of the NDVI [25].

Hay yield monitor was used to collect the hay yields for alfalfa and Rhodes grass. A hay yield monitor Model 880 of

TABLE IV
CHARACTERISTICS OF ASTER DATA USED FOR THE STUDY

Acquisition date	Julian day	Sun earth distance (Astronomic unit)	Azimuth angle (°)	Sun elevation angle (°)	Zenith angle (°)	Acquisition date	Julian day	Sun earth distance (Astronomic unit)	Azimuth angle (°)	Sun elevation angle (°)	Zenith angle (°)
Feb. 17, 2012	48	0.98814	147.2297	48.276794	41.723206	Aug. 4, 2012	217	1.01444	105.1021	68.75347	21.24653
Mar. 4, 2012	64	0.99183	143.0621	53.407243	36.592757	Sep. 12, 2012	256	1.0062	137.3152	64.274601	25.725399
Mar. 20, 2012	80	0.99612	138.3307	59.121105	30.878895	Oct. 7, 2012	281	0.99918	148.8947	55.917377	34.082623
Apr. 21, 2012	112	1.00519	121.7621	69.281025	20.718975	Nov. 15, 2012	320	0.98894	160.7625	45.355277	44.644723
June 1, 2012	153	1.01418	93.1412	72.072651	17.927349	Feb. 13, 2013	43	0.98717	146.5748	45.87058	44.12942
Jun. 17, 2012	169	1.01603	89.0599	71.482986	18.517014	Mar. 16, 2013	75	0.99474	137.4705	56.622189	33.377811
Jul. 3, 2012	185	1.0167	89.5028	70.644245	19.355755	May 19, 2013	123	1.00806	113.7682	71.434647	18.565353
Jul. 19, 2012	201	1.01616	95.0762	69.843022	20.156978						

Harvest Tech., USA, was installed on a large square baler (Claas 3000) for recording the CP data at the time of baling. The hay yield maps were prepared by interpolating the filtered point data to 4 m × 4 m grids using an ordinary kriging tool of ESRI GIS (ver. 2010) [26]. During the preparation of the hay yield maps, low- or high-yielding points associated with significant turning and manoeuvring of the baler were removed [27], as were the short segments, which were affected by start or end-pass delays [28].

2) Water Use Mapping: WUM was accomplished by using crop ET and assuming that the amount of water used by crops was equal to seasonal ET (ETactual). The SEBAL method was used to compute the ETactual on a pixel-by-pixel basis for the instantaneous time of satellite image as the residual amount of energy remaining from the classical energy balance (2) [9]

$$\lambda ET = R_n - G - H \qquad (2)$$

where λET is the latent heat flux (an instantaneous value for the time of the satellite overpass), R_n is the net radiation at the surface, G is the soil heat flux [calculated using (11)], and H is the sensible heat flux to the air [calculated using (12)]. The unit for all fluxes was $W/m^2/day$. The SEBAL computes λET as a "residual" of net radiant energy after G and H are subtracted.

The first step in the SEBAL procedure is to compute R_n by using the surface radiation balance equation (3)

$$R_n = (1 - \propto)R_{s\downarrow} + R_{L\downarrow} - R_{L\uparrow} - (1 - \varepsilon_0)R_{L\downarrow} \qquad (3)$$

where R_n is the net radiation at the surface, α is the surface albedo, $R_{s\downarrow}$ is the incoming short-wave radiance, $R_{L\downarrow}$ is the incoming long-wave radiance, $R_{L\uparrow}$ is the outgoing long-wave radiation, and ε_0 is the surface emissivity. All of these parameters were accomplished in a series of steps using the ERDAS Imagine model maker tool as described in the SEBAL manual [29].

Surface albedo: Georectified ASTER VNIR bands were subjected to Top-Of-Atmosphere (TOA) reflectance. This enabled the conversion of image digital numbers (DN) to at-sensor radiance (L_λ) and subsequently to spectral reflectance (ρ_λ) by adopting the procedures of the ASTER User Manual [20]. The spectral reflectance of each band was then used to compute the Albedo-top of the atmosphere (α_{TOA}) by utilizing the two visible band albedos (4) of Liang [30] and the computed surface albedo (α) by correcting the α_{TOA} (5)

$$\alpha_{visible} = 0.8845\alpha_1 + 0.122\alpha_2 - 0.0158 \qquad (4)$$

where α_1 and α_2 are the VNIR 1 and VNIR 2 bands of the ASTER image, respectively, and

$$\propto = \frac{\alpha_{TOA} - \alpha_{path\_radiance}}{\tau_{sw}^2} \qquad (5)$$

where the path radiance is the average portion of the incoming solar radiation across all bands that is back-scattered to the satellite before it reaches the earth's surface and τ_{sw} is the atmospheric transmissivity. In this study, α path-radiance value was considered as 0.03 [31]. The τ_{sw} values assume clear sky and relatively dry conditions and are obtained by using an elevation-based relationship: $\tau_{sw} = 0.75 + 2 \times 10^{-5} \times z$ [32], where z is the elevation of the weather station above sea level (m).

Incoming short-wave radiation ($R_{s\downarrow}$): The incoming short-wave radiation is the direct and diffused solar radiation flux that actually reaches the earth's surface (W/m^2); this was calculated assuming clear sky conditions as a constant for the entire image (6)

$$R_{s\downarrow} = G_{sc} * COS\theta * d * \tau_{sw} \qquad (6)$$

where G_{sc} is the solar constant (1367 W/m^2), $cos\theta$ is the cosine of the solar incidence angle, d is the inverse squared relative earth-sun distance, and τ_{sw} is the atmospheric transmissivity.

Outgoing long-wave radiation ($R_{L\uparrow}$): The outgoing long-wave radiation is the thermal radiation flux emitted from the earth's surface to the atmosphere (W/m^2); this was computed by applying the Stefan–Boltzmann equation (7)

$$R_{L\uparrow} = \varepsilon_o * \sigma * T_s^4 \qquad (7)$$

where ε_o is the broad-band surface emissivity (dimensionless), σ is the Stefan–Boltzmann constant ($5.67 \times 10^{-8} W/m^2/K^4$), and T_s is the surface temperature (K). The surface emissivity (ε_o) was computed using an empirical equation where the NDVI > 0 by inputting the NDVI and the LAI, as described in the SEBAL user manual [29]. Subsequently, the surface temperature (T_s) was computed from the ASTER TIR band 13 [21] and used in the computations.

Incoming long-wave radiation ($R_{L\downarrow}$): The incoming long-wave radiation is the downward thermal radiation flux from the atmosphere (W/m^2) that was computed using the Stefan–Boltzmann equation (8)

$$R_{L\downarrow} = \varepsilon_a * \sigma * T_a^4 \qquad (8)$$

TABLE V
SUMMARY OF GROUND MEASURED NDVI AND LAI

Growth cycle	Crop	Season/year	$NDVI_{(G)}$			$LAI_{(G)}$		
			Mean	SD	Range	Mean	SD	Range
Annual crops	Corn	2012	0.71	0.19	0.49–0.81	4.37	1.48	2.48–5.46
		2013	0.63	0.17	0.42–0.75	4.43	1.46	2.83–6.04
	Wheat	2012	0.63	0.10	0.42–0.75	4.74	1.31	3.79–5.59
		2013	0.60	0.15	0.36–0.74	2.60	1.05	0.21–4.98
	Barley	2012	NA	NA	NA	NA	NA	NA
		2013	0.58	0.28	0.42–0.72	3.40	1.28	2.97–4.12
Biennial crops	Alfalfa	2012	0.62	0.17	0.42–0.82	4.51	1.74	2.68–6.24
		2013	0.51	0.12	0.12–0.81	4.02	1.33	1.89–6.19
	Rhodes grass	2012	0.65	0.16	0.25–0.81	4.50	1.54	2.06–5.91
		2013	0.22	0.06	0.16–0.29	1.00	0.24	0.91–1.19

TABLE VI
NDVI MODELS USED FOR PREDICTING CROP PRODUCTIVITY

Sl. No	Crop	Julian day	Model	R^2		RMSE (Yield t/ha)	
				Modeled	Cross-validated	Modeled	Cross-validated
1	Alfalfa	281 (2012)	$Y = 9.6754 * NDVI - 0.1097$	0.5821 (P>0.028)	0.6821 (P>0.047)	986 (21%)	1211 (19%)
2	Barley	43 (2013)	$Y = 8.8221 * NDVI - 1.1621$	0.6214 (P>0.021)	0.6682 (P>0.034)	1567 (16%)	1687 (19%)
3	Corn	169 (2012)	$Y = 21.4579 * NDVI - 1.6884$	0.5647 (P>0.031)	0.711 (P>0.038)	2218 (18%)	2788 (21%)
4	Rhodes grass	201 (2012)	$Y = 11.3946 * NDVI - 0.3807$	0.5211 (P>0.046)	0.5711 (P>0.039)	1087 (24%)	1372 (22%)
5	Wheat	64 (2012)	$Y = 13.821 * NDVI - 6.0231$	0.6211 (P>0.021)	0.6822 (P>0.038)	1086 (15%)	1124 (17%)

where ε_a is the atmospheric emissivity (dimensionless), σ is the Stefan–Boltzmann constant ($5.67 \times 10^{-8} W/m^2/K^4$), and T_a is the near surface air temperature (K). ε_a was calculated using (9) [23]

$$\varepsilon_a = 0.85 * (-\ln \tau_{sw})^{0.09} \tag{9}$$

where τ_{sw} is the atmospheric transmissivity.

Substituting (9) into (8) and using T_{cold} from the selected cold pixel for T_a provides the following equation (10):

$$R_{L\downarrow} = 0.85 * (-\ln T_{sw})^{0.09} * \sigma * T_{cold}^4 \tag{10}$$

Two anchor (hot and cold) pixels were selected [29] to fix boundary conditions for the energy balance. The cold pixel was selected as a wet, well-irrigated crop surface having full ground cover by vegetation. The surface temperature and near-surface air temperature were assumed to be similar at this pixel. The hot pixel was selected as a dry, bare agricultural field where ET was assumed to be zero.

Soil heat flux (G): G is the rate of heat storage into the soil and vegetation due to conduction. It was obtained by using the empirical equation (11) representing values near midday [34]

$$G = \left[\frac{T_s - 273.16}{\propto}(0.0038 \propto + 0.007 \propto^2)(1 - 0.98 NDVI^4)\right] R_n \tag{11}$$

where T_s is the surface temperature (°C), α is the surface albedo, the NDVI is the Normalized Difference Vegetation Index, and R_n is the net surface radiation flux.

Sensible heat flux (H): The H is the rate of heat loss to the air by convection and conduction due to a temperature difference. It was computed by using (12) for heat transport

$$H = \frac{\rho * C_p * \Delta T}{r_{ah}} \tag{12}$$

where ρ is the air density (kg/m^3), C_p is the specific heat of air (1004 J/kg/K), ΔT (K) is the temperature difference, and r_{ah} is the aerodynamic resistance to heat transport (s/m). Therefore, H is a function of the temperature gradient, surface roughness, and

TABLE VII
PHENOLOGY OF BIENNIAL CROPS CORRESPONDING TO ASTER IMAGE
ACQUISITION DATES

ASTER image acquisition date	Pivot no.	Harvest date	Age corresponding to ASTER image (days)
Alfalfa			
Oct 7, 2012 (JD 281)	TE-10	Oct. 7, 2012	0
	TE-03	Oct. 6, 2012	1
	TE-05, TE-06	Oct. 3, 2012	4
	LN-1	Sep. 28, 2012	9
	10	Sep. 18, 2012	19
	TE-01	Sep. 17, 2012	20
	TE-02	Sep. 16, 2012	21
	25, 1–5	Sep. 14, 2012	23
	12B, 12C	Sep. 11, 2012	26
	TE-04, TE-07	Sep. 10, 2012	27
	TE-08	Aug. 17, 2012	51
Rhodes grass			
Jul. 19, 2012 (JD 201)	3, TE-09	Jul. 18, 2012	1
	4	Jul. 17, 2012	2
	21	Jul. 16, 2012	3
	2, 5–5	Jul. 15, 2012	4
	Feb. 5	Jul. 13, 2012	6
	6	Jul. 12, 2012	7
	17	Jul. 11, 2012	8
	18	Jun. 22, 2012	27
	26	Jun. 5, 2012	44
	23	Jun. 3, 2012	46
	13, 20	Jun. 2012	47
	14, 3–5	May 28, 2012	52
	11, 15, 16	May 27, 2012	53
	7, 8, 12A	May 26, 2012	54
	TE11	May 24, 2012	56
	22, 21S	May 16, 2012	64
	4–5, 6TDF	May 15, 2012	65
	21A	May 12, 2012	68

TABLE VIII
PHENOLOGY OF ANNUAL CROPS CORRESPONDING TO ASTER IMAGE
ACQUISITION DATES

Image acquisition date	Crop	Pivot no.	Date of sowing	Age corresponding to ASTER image (days)
Feb. 13, 2013 (JD 43)	Barley	11, 2–5, 4–5	Dec. 18, 2012	57
		5, 15	Dec. 12, 2012	63
		17, 18	Dec. 9, 2012	66
		25, 21S, TE-09	Dec. 6, 2012	69
Mar. 4, 2012 (JD 64)	Wheat	TE-11	Jan. 1, 2012	63
		11,14,26	Dec. 19, 2011	76
		LIN-2, PAL	Dec. 6, 2011	89
		4, 18	Nov. 28, 2011	97
Jun. 17, 2012 (JD 169)	Corn	PAL	Apr. 30, 2012	48
		LN-2	Apr. 2, 2012	76

This is the energy equivalent of the instantaneous ET at the time of satellite overpass. The evaporative fraction (EF) for each pixel was calculated.

The λET, i.e., the rate of LE loss from the surface due to ET, is considered an instantaneous value for the time of satellite overpass used to compute instantaneous ET (ET_{inst}) and reference evaporative fraction (ET_rF) values by applying (13) and (14)

$$ET_{inst} = 3600 \frac{\lambda ET}{\lambda} \qquad (13)$$

where ET_{inst} is the instantaneous ET (mm/h), 3600 is the time conversion from seconds to hours, and λ is the latent heat of vaporization or the heat observed when a kilogram of water evaporates (J/kg); and

$$ET_rF = \frac{ET_{inst}}{ET_r} \qquad (14)$$

where ET_{inst} derives from (13) (mm/h) and ET_r is the crop-coefficient (K_c) of a known crop. This study considers the K_c of alfalfa as the ET_r at the time of the image overpass. The daily values of ET (ET_{24}, mm/day) were computed using (15) and then extrapolated to a growing season or for a particular period employing (16), as described in the SEBAL manual [29]

$$ET_{24} = ET_rF * ET_{r\_24} \qquad (15)$$

where ET_{r_24} is the cumulative 24-h ET_r for the day of the image, which is calculated by adding the hourly ET_r values over the day of the image and ET_rF is the reference evaporative fraction

$$ET_{season} = ET_rF_{season} \sum_{1}^{n} ET_{r\_24} \qquad (16)$$

where the ET_rF_{season} is the representative ET_rF for the growing season or period, ET_{r_24} is the daily ET_r, and n is the number of days in the period. Units for ET_{season} are computed in mm, whereas the ET_{r_24} is in mm/day.

wind speed. Equation (12) is difficult to solve because of two unknowns $-r_{ah}$ and ΔT. To facilitate this computation, we utilized the two selected "anchor" pixels (where reliable values for H can be predicted and a ΔT estimated) and the wind speed at a given height (which was obtained from the weather station) as described in the SEBAL manual [29].

The SEBAL procedure (2) was completed by computing the net surface radiation flux (R_n) using the surface radiation balance equation (3), the soil heat flux (11), and the sensible heat flux (12). After R_n, G, and the final value of H were established, the latter after an iterative process to consider atmospheric stability effects, the Latent Heat (LE) was then calculated as a residual.

TABLE IX
PREDICTED AND ACTUAL CROP PRODUCTIVITY, EVAPOTRANSPIRATION/WATER USE AND WATER PRODUCTIVITY

Crop	Year/season	Predicted			Actual		
		CP_P (kg/ha)	ET_P (m^3/ha)	WP_P (kg/m^3)	CP_A (kg/ha)	WA (m^3/ha)	WP_A (kg/m^3)
Corn	2012-Season 1	13510 (±3020)	9050	1.49 (± 0.14)	10930 (±1940)	9892	1.11 (± 0.09)
	2012-Season 2	14060 (±2710)	14013	1.00 (± 0.12)	11190 (±2090)	18242	0.61 (± 0.08)
	2013-Season 1	12690 (±2980)	22962	0.55 (± 0.16)	10900 (±2710)	21580	0.51 (± 0.12)
Wheat	2012-Season 1	6000 (±520)	7517	0.80 (± 0.02)	5530 (±680)	4831	1.15 (± 0.03)
	2013-Season 1	7370 (±380)	3667	2.01 (± 0.03)	6510 (±620)	3982	1.63 (± 0.02)
Barley	2012-Season 2	7210 (±420)	10648	0.68 (± 0.04)	6910 (±1120)	12594	0.55 (± 0.02)
Alfalfa	2012	42450 (±6230)	94890	0.46 (± 0.04)	35100 (±5840)	84852	0.41 (± 0.04)
	2013	15530 (±3160)	40566	0.38 (± 0.01)	21000 (±2720)	48641	0.43 (± 0.02)
Rhodes grass	2012	58210 (±10430)	168224	0.36 (± 0.03)	60390 (±5440)	163294	0.37 (± 0.04)
	2013	24580 (±4220)	23022	1.07 (± 0.07)	15140 (±3220)	22053	0.69 (± 0.02)

CP_P, ASTER predicted crop productivity; ET_P, ASTER predicted evapotranspiration; WP_P, ASTER predicted water productivity; CP_A, TAF recorded crop productivity; WA, Actual quantity of water applied; WP_A, actual water productivity.

III. RESULTS

A. $NDVI_{(G)}$ and $LAI_{(G)}$

The $NDVI_{(G)}$ and $LAI_{(G)}$ were examined across the crops during the study period (Table V). The $NDVI_{(G)}$ values ranged between 0.12 (initial stage) and 0.82 (canopy closure stage). The $NDVI_{(G)}$ value of alfalfa was 0.62 (±0.17) and 0.51 (±0.12) in 2012 and 2013, respectively. Meanwhile, Rhodes grass recorded a high $NDVI_{(G)}$ value of 0.65 in 2012 and the least $NDVI_{(G)}$ value of 0.22 in 2013. The $NDVI_{(G)}$ of seasonal crops ranged between 0.63 (wheat) and 0.71 (corn) in 2012; however, it varied from 0.53 (barley) to 0.63 (corn) in 2013. The $LAI_{(G)}$ varied between 0.21 (initial stage) and 6.04 (canopy closure stage). The $LAI_{(G)}$ in the alfalfa crop was 4.51 (±1.74) and 4.02 (±1.33) in 2012 and 2013, respectively, whereas the $LAI_{(G)}$ for Rhodes grass was 4.50 (±1.54) and 1.00 (±0.24) in 2012 and 2013, respectively. In the annual crops, a higher $LAI_{(G)}$ was observed in wheat (4.74 ± 1.31), followed by corn (4.37 ± 1.48) during the year 2012. However, in 2013, corn recorded a higher $LAI_{(G)}$ (4.43 ± 1.46) compared to barley (3.40 ± 1.28) and wheat (2.60 ± 1.05).

B. CP Models

The best relationship between CP and NDVI was obtained when the crops were in mid-season (growth stage), as presented in Table VI. In the annual crops, the best response was observed on the Julian days of 43 (2013), 169 (2012), and 64 (2012) for barley, corn, and wheat crops, respectively, when the crops were at their peak growth stage. In the biennial crops (alfalfa and Rhodes grass), which have a growth period of 30 to 45 days between the two harvests, the best response was observed on the

Julian day 201 and 281 of 2012 for Rhodes grass and alfalfa, respectively (Tables VII and VIII).

The CP models were validated against the actual CP data recorded on the farm; there was good correlation (Table VI). The root mean square error (RMSE) between the farm recorded and model predicted CP was high in Rhodes grass (24%), followed by alfalfa (21%), corn (18%), and barley (16%), with the least RMSE observed in wheat (15%). However, similar RMSE values were observed in the cross-validation of the models (Table VI).

C. CP (kg/ha/season)

The results of the predicted and actual ET/crop water use CP and WP for both annual and biennial cops are presented in Table IX. It was observed that predicted CP (CP_P) varied significantly in both temporal and spatial scales. For annual crops, the average CP_P for corn was 13 510 and 14 060 for season 1 and 2, respectively, in 2012 and 12 690 in 2013. However, the actual recorded CP (CP_A) for corn was 10 930 and 11 190 for season 1 and 2, respectively, in 2012, and 10 900 in 2013. Meanwhile, the average CP_P for the wheat crop was 6000 and 7370 for season 1 in 2012 and 2013, respectively. But, the CP_A for the wheat crop was 5530 and 6510 for season 1 in 2012 and 2013, respectively. In the case of barley, the farm recorded mean CP_A was 7210 kg/ha, whereas the CP_P was 6910 kg/ha, resulting in a mean error of 4.16%.

For the biennial crops, the CP_P (kg/ha/year) for alfalfa was 42 450 for 2012 and 15 530 for 2013 (up to May 19). The CP_A for the alfalfa crop was 35 100 for 2012 and 21 000 for 2013. Although the average CP_P for Rhodes grass was 58 210 for 2012 and 24 580 for 2013 (up to May 19), the CP_A for Rhodes grass was 60 390 for 2012 and 15 140 for 2013.
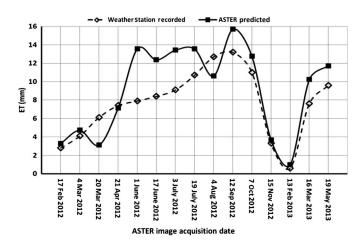
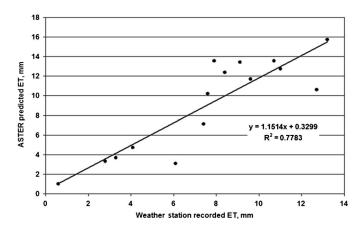Fig. 3. Temporal variation in ASTER predicted (ET_P) and weather station recorded ET (ET_W).

Fig. 4. Regression between ASTER predicted (ET_P) and weather station recorded ET (ET_W).

D. Water Use (ET) Mapping

ET values were estimated in this study through the analysis of ASTER images using the SEBAL model. The accuracy of the ASTER predicted ET (ET_p) data using the SEBAL model was tested against the weather station recorded ET (ET_w) data. The distribution pattern of ET_p and ET_w is illustrated in Fig. 3. Both the ET_p and ET_w followed a similar pattern throughout the study period. The correlation between ET_p and ET_w was further investigated through the regression analysis technique. The results showed a strong linear relationship between ET_p and ET_w, with an R^2 of 0.78 (Fig. 4). The mean deviation of the ET_p from the ET_w was found to be 10.49%. The ET_p (Fig. 5) was then used to assess IP for all of the test crops. The mean values of both ET_p and the actual quantity of irrigation WA are presented in Figs. 6 and 7.

During the 2011–2012 season, the WA to alfalfa, Rhodes grass and wheat crops was lower than the required quantity as per the ET_p. However, during the 2012–2013 season, alfalfa, wheat, and barley crops were irrigated with more than the required quantity of water. Conversely, corn received a higher than required quantity of water during 2011–2012 and a lower than required quantity during 2012–2013.

The deviation of ET_p from the WA to all of the crops was determined in terms of overall mean error (Fig. 8). The results
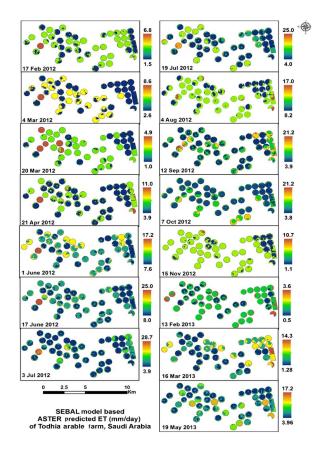

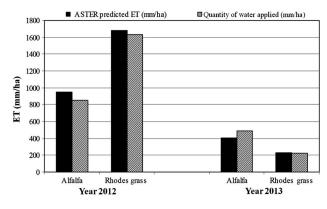Fig. 5. SEBAL model-based ASTER predicted ET (mm/day) for the study site.

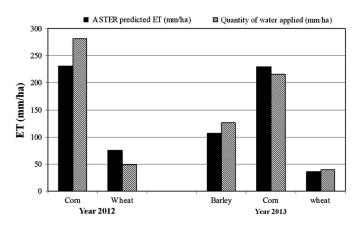Fig. 6. ASTER predicted ET (ET_P) and the water applied (WA) to biennial crops.

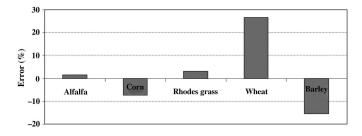Fig. 7. ASTER predicted ET (ET_P) and the water applied (WA) to annual crops.

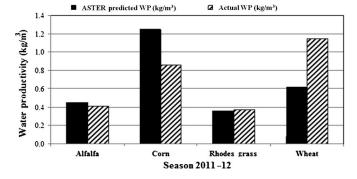Fig. 8. Accuracy assessment of predicted ET (ET$_P$) vs. Water applied (WA).

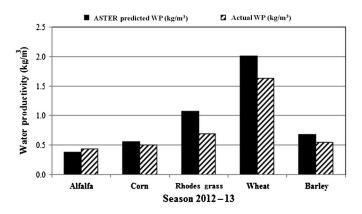Fig. 9. ASTER predicted (WP$_P$) vs. Actual (WP$_A$) water productivity for 2012.

Fig. 10. ASTER predicted (WP$_P$) vs. Actual (WA$_A$) water productivity for 2013.

indicated that the accuracy of ET$_p$ was higher for alfalfa, corn, and Rhodes grass crops and lower for wheat and barley.

E. Water Productivity

As depicted in Fig. 9, the prediction of WP (WP$_p$) was more accurate for alfalfa and Rhodes grass crops in 2012. In alfalfa, the WP$_p$ was 0.46 kg/m^3 versus an actual WP (WP$_A$) of 0.41 kg/m^3. Meanwhile, the WP$_p$ for Rhodes grass was 0.36 kg/m^3 versus a WP$_A$ of 0.37 kg/m^3. In 2013 (Fig. 10), the WP$_p$ was 2.01, 1.07, 0.68, 0.55, and 0.38 kg/m^3 for wheat, Rhodes grass, barley, corn, and alfalfa, respectively, versus WP$_A$ values of 1.63, 0.69, 0.55, 0.51, and 0.43 for the same sequence of crops.

IV. DISCUSSION AND CONCLUSION

As indicated by the regression models, the CP of all the crops showed a visible and significant trend across a range of NDVI values. The R^2 values were moderate and ranged from 0.5211

(Rhodes grass) to 0.6214 (corn). This is one of the drawbacks of statistical expressions for relationships between the NDVI and the CP [35]. This was also evident in the cross-validation of the models, where the CP data were particularly inconsistent for forage crops due to bias in the selection of the proper growth stage (duration between two harvests) for the CP predictions. Conversely, the seasonal performance of different species, phenology, spectral response, and the establishment of time-dependent relationships with crop vigour and productivity played a major role in developing yield models [36], [37]. Despite this, the obtained R^2 values concurred with the earlier reported values. For example, in the case of the corn crop, the strong relationship of the NDVI and the CP estimates occurred in the June (i.e., Julian day, 169) image, with an R^2 value of 0.5647; this was considerably higher than the reported values (R^2 = 0.16−0.38) in a previous study [38], but lower than that reported in another study (R^2 = 0.78) [39]. This research gained further support from previous studies on wheat crop, where the lowest CP prediction accuracy was obtained; accurate wheat CP predictions were possible using only one image, provided the image was acquired toward the middle of the growing season when most wheat [40] and corn [41] crop canopies were fully developed.

The results of this study showed that spatial distribution of ET could be predicted with an overall accuracy of 90%. The results of the ET$_p$ concur with the results of another study that used the SEBAL model to estimate ET in the Philippines, where the ET values deviated by 9% from the ETc (Penman-Monteith) for the ASTER sensor [42]. The obtained results were better than expected, as most remote sensing techniques used for estimating evaporation (E) have accuracies of 70%–85% compared with ground-based measurements [9]. In another study that summarized the accuracy of ET prediction using the SEBAL model (although under different climatic conditions), the accuracy at field scale was 85% for 1 day and reached 95% on a seasonal basis, whereas the average accuracy of annual ET for large watersheds was observed to be 96% [14].

On an annual/seasonal basis, a deviation of approximately 19% was observed between the ET$_P$ and ET$_w$. When focusing on a finer timescale, the model resulted in a large deviation (i.e., −49% to +63%). The model overestimated the ET$_P$ for the ASTER images of June 1, 2012 (63%); June 17, 2012 (47%); July 3 (47%); February 13 (63%); and March 16, 2013 (34%), whereas underestimated the ET$_P$ for the March 20, 2012 (49%); April 21, 2012 (4%); and August 4, 2012 (16%) images. This might be due to the gradation of individual pixels' evaporative response, which can reflect upon the diversity of crops, growth stages, and gradients in soil moisture conditions across the fields [43], [44].

The WP of alfalfa observed in this study (0.38−0.43 kg/m^3) concurred with the previously reported values (0.18−0.60 kg/m^3) [45]. The harvests made in the cooler months of January–March 2012, November 2012, and February 2013 recorded a higher WP (0.63−0.81 kg/m^3) than the harvests made in warmer months (i.e., 0.23–0.40). It is evident that alfalfa, being a C$_3$ plant, is adapted to cuttings made in cooler seasons but loses its efficiency during the summer season [46]. This large amount of variation may be attributed to the influence of both spatial and seasonal climatic variations on ET, alfalfa productivity, and water use efficiency. Similar results were reported
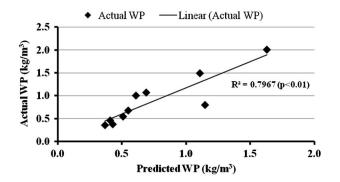
Fig. 11. Regression between predicted (WP$_P$) vs. Actual (WA$_A$) water productivity.

when comparisons were made between CP and ET for individual harvests, where the relationship varied across the growing season and changed depending on the harvest time [47]. A better correlation between the WP$_P$ and field recorded WP$_A$ for the entire farm was observed, with an R^2 of 0.7967 (p < 0.01) as shown in Fig. 11. Meanwhile, among the three annual crops, there were considerable differences between the WP$_P$ and WP$_A$ in wheat and barley (C$_3$ plants) but not in corn (C$_4$ plant). In the case of wheat, the WP$_P$ (kg/m^3) values of 0.80–2.01 closely resembled the WP$_A$ values of 0.1–2.07 [48], but were higher than the values of 0.51–1.50 reported by others [49]–[52]. The lower WP observed in the earlier studies could be due to the lower CP of 4.3–4.88 t/ha [49], [50] compared to 6.0 t/ha in the present study. For corn, the WP$_P$ (0.55−1.49 kg/m^3) concurred with the WP (1.01 kg/m^3) reported earlier from Iran [53]. However, there were other reports with much higher WP values of 0.82−4.5 kg/m^3 [54], [55]. The WP values of 0.44−1.07 kg/m^3 observed in Rhodes grass resembled earlier reported values of 0.7 kg/m^3 [56] and 0.53−0.85 kg/m^3 [57], but were lower than the values (1.18−2.13 kg/m^3) reported by ICARDA [58]. In the case of barley, the WP$_P$ and WP$_A$ values were 0.68 ($\pm$0.04) and 0.55 ($\pm$0.02) kg/m^3, respectively. The values were within the range of values reported in Mediterranean environments [59], [60].

The performance of the prediction models was assessed against the recorded/measured data (Table X). The overall percentage bias values for CP, ET, and WP were 9.4%, −2.68%, and 9.65%, respectively, whereas the RMSE values were 1996 (kg/ha), 2107 (m^3/ha), 0.087 (kg/m^3) for CP, ET, and WP, respectively. When converted into variations between the actual and the predicted CP, the variations were 8%–12% for wheat, 14%–20% for corn, 4% for barley, 17%–35% for alfalfa, and 3%–38% for Rhodes grass. Although the performance of the models varied among crops and across seasons/years, the prediction bias values were within acceptable limits.

Based on the results of this study, it can be inferred that WP of wheat was consistently higher than all the other studied crops. Further, among the fodder crops, corn recorded higher WP compared to extensively cultivated crops such as alfalfa and Rhodes grass. The results of this research work were shared with few agricultural companies. As a result, there was a shift in the cropping pattern on TAF in 2013, wherein the area under corn increased and the area under Rhodes grass decreased as compared to the previous year.

TABLE X
MODEL PERFORMANCE ASSESSMENT PARAMETERS

Year	Crop	Season	Root mean square error (RMSE)			Percentage bias (PBIAS)		
			CP (kg/ha)	ET (m^3 / ha)	WP (kg / m^3)	CP (%)	ET (%)	WP (%)
2012	Corn	Season 1	2864	746	0.17	19.10	−9.30	25.50
		Season 2	1298	1371	0.14	20.41	−30.18	39.00
	Wheat	Season 1	1565	345	0.03	07.83	35.73	−43.75
	Alfalfa		1535	835	0.02	17.31	10.58	10.87
	Rhodes grass		1501	696	0.03	−3.75	02.93	−2.78
2013	Corn	Season 1	3593	2567	0.21	14.11	06.02	07.27
	Wheat	Season 1	1265	3466	0.11	11.67	−8.59	18.91
	Barley	Season 2	2601	4453	0.05	04.16	−18.28	19.12
	Alfalfa		1074	3888	0.08	−35.22	−19.91	−13.16
	Rhodes grass		2666	2708	0.03	38.41	04.21	35.51
	Overall		1996	2107	0.09	09.40	−2.68	09.65

This study also concludes that the SEBAL algorithm using ASTER images provided realistic estimates of ET, CP, and WP for the crops (corn, wheat, barley, Rhodes grass, and alfalfa) cultivated under center-pivot irrigation system in Saudi Arabia. There was concurrence between the predicted and actual values of CP and WP. However, the predicted daily ET values significantly deviated from the meteorological data, particularly in summer months (June–September); this issue warrants further empirical research.

APPENDIX I

ASTER SATELLITE SYSTEM: SENSOR CHARACTERISTICS

Particulars	VNIR	SWIR[a]	TIR
Bands	1–3	4–9	10–14
Spatial resolution	15 m	30 m	90 m
Swath width	60 km	60 km	60 km
Cross track pointing	±318 km (±24°)	±116 km (±8.55°)	±116 km (±8.55°)
Quantization (bits)	8	8	12

VNIR, visible and near infrared; SWIR, shortwave infrared; TIR, thermal infrared.
[a]SWIR data invalid as of April 2008. [20].

REFERENCES

[1] K. R. Calzadilla and R. S. J. Tol, "The economic impact of more sustainable water use in agriculture: A computable general equilibrium analysis," J. Hydrol., vol. 384, no. 3–4, pp. 292–305, 2010.

[2] C. De Fraiture and D. Wichelns, "Satisfying future water demands for agriculture," *Agric. Water Manage.*, vol. 97, no. 4, pp. 502–511, 2010.

[3] P. Droogers *et al.*, "Water resources trends in Middle East and North Africa towards 2050," *J. Hydrol. Earth Syst. Sci.*, vol. 16, pp. 1–14, 2012.

[4] F. Trieb and H. Muller-Steinhagen, "Concentrating solar power for seawater desalination in the Middle East and North Africa," *Desalination*, vol. 220, pp. 165–168, 2008.

[5] Food and Agriculture Organization (FAO), "Water profile of Saudi Arabia," in *Encyclopedia of Earth*, A. K. Panikkar, Ed., 2008 [Online]. Available: http://www.eoearth.org/article/Water_profile_of_Saudi_Arabia, accessed on Aug. 27, 2013.

[6] R. L. Hanson, "Evapotranspiration and droughts," in *National Water Summary 1988–89: Hydrologic Events and Floods and Droughts (U.S. Geological Survey Water-Supply Paper 2375)*, R. W. Paulson, E. B. Chase, R. S. Roberts and D. W. Moody, Eds., Denver, CO, USA: United States Govt. Printing Press/USGS, 1991, pp. 99–104.

[7] K. M. P. S. Bandara, "Monitoring irrigation performance in Sri Lanka with high-frequency satellite measurements during the dry season," *Agric. Water Manage.*, vol. 58, pp. 159–170, 2003.

[8] M. Ozdogan, Y. Yang, G. Allez, and C. Cervantes, "Remote sensing of irrigated agriculture: Opportunities and challenges," *Remote Sens.*, vol. 2, pp. 2274–2304, 2010.

[9] W. G. M. Bastiaanssen *et al.*, "SEBAL model with remotely sensed data to improve water-resources management under actual field conditions," *J. Irrig. Drain. Eng.*, vol. 131, pp. 85–93, 2005.

[10] G. J. Roerink, Z. Su, and M. Menenti, "S-SEBI: A simple remote sensing algorithm to estimate the surface energy balance—Physics and chemistry of the earth. Part B," *Hydrol. Ocean Atmos.*, vol. 25, no. 2, pp. 147–157, 2000.

[11] G. B. Senay *et al.*, "Operational evapotranspiration mapping using remote sensing and weather datasets: A new parameterization for the SSEB approach," *J. Amer. Water Resour. Assoc.*, vol. 49, no. 3, pp. 577–591, 2013.

[12] R. G. Allen, M. Tasumi, and R. Trezza, "Satellite-based energy balance for mapping evapotranspiration with internalized calibration (METRIC)-model," *J. Irrig. Drain. Eng.*, vol. 133, no. 4, pp. 380–394, 2007.

[13] S. J. Zwart and W. G. M. Bastiaanssen, "SEBAL for detecting spatial variation of water productivity and scope for improvement in eight irrigated wheat systems," *Agric. Water Manage.*, vol. 89, pp. 287–296, 2007.

[14] J. D. Kalma, T. R. McVicar, and M. F. McCabe, "Estimating land surface evaporation: A review of methods using remotely sensed surface tempera-ture data," *Surv. Geophys.*, vol. 29, pp. 421–469, 2008.

[15] M. Akbari, N. Toomanian, P. Droogers, W. Bastiaansssen, and A. Gieske, "Monitoring irrigation performance in Esfahan, Iran, using NOAA satellite imagery," *Agric. Water Manage.*, vol. 88, pp. 99–109, 2007.

[16] B. S. Karatas, E. Akkuzu, H. B. Unal, S. Asik, and M. Avci, "Using satellite remote sensing to assess irrigation performance in Water User Associations in the Lower Gediz Basin, Turkey," *Agric. Water Manage.*, vol. 96, no. 6, pp. 982–990, 2009 [Online]. Available: http://www.sciencedirect.com/science/journal/03783774

[17] W. G. M. Bastiaanssen *et al.*, "Historic groundwater abstractions at national scale in the Kingdom of Saudi Arabia," *Rep. Water Watch*, Ministry of Water and Electricity, Riyadh, Saudi Arabia, 2006.

[18] World Water Assessment Programme (WWAP), "The United Nations world water development report 4: Managing water under uncertainty and risk," UNESCO, Paris, France, Tech. WWDR4, 2012, vol. 1, 85 pp.

[19] K. H. Alzahrani, S. E. Muneer, A. S. Taha, and M. B. Baig, "Appropriate cropping pattern as an approach to enhancing irrigation water efficiency in the Kingdom of Saudi Arabia," *J. Anim. Plant Sci.*, vol. 22, no. 1, pp. 224–232, 2012.

[20] M. Abrams, S. Hook, and B. Ramachandran, *ASTER User Handbook—Ver. 2*, Jet Propulsion Lab., California Inst. Technol., NASA, USA, p. 135 [Online]. Available: http://asterweb.jpl.nasa.gov/content/03_data/04_Documents/aster_ user_guide_v2.pdf, accessed on Sep. 11, 2012.

[21] A. Ghulam, *How to Calculate Reflectance and Temperature using ASTER data?* St. Louis, MO, USA: Center for Environmental Sciences, Saint Louis Univ., 2009 [Online]. Available: http://www.gis.slu.edu/RS/ASTER_Re-flectance_Temperature_Calculation.php, accessed on Sep. 25, 2012.

[22] J. W. Rouse, R. H. Haas, J. A. Schell, and D. W. Deering, "Monitoring vegetation systems in the Great Plains with ERTS," in *Proc. 3rd ERTS Symp.*, 1973, vol. 1, pp. 309–317.

[23] A. Platonov *et al.*, "Water productivity mapping (WPM) using Landsat ETM+ data for the irrigated croplands of the Syrdarya River Basin in Central Asia," *Sensors*, vol. 8, pp. 8156–8180, 2008.

[24] S. M. E. Groten, "NDVI-crop monitoring and early yield assessment of Burkina Faso," *Int. J. Remote Sens.*, vol. 14, pp. 1495–1515, 1993.

[25] D. Xin, B. Wu, Q. Li, J. Meng, and K. Jia, "A method to estimate winter wheat yield with the MERIS data," in *Proc. PIERS*, Beijing, China, Mar. 23–27, 2009, pp. 1392–1395.

[26] A. Dobermann, J. L. Ping, V. I. Adamchuk, G. C. Simbahan, and R. B. Ferguson, "Classification of crop yield variability in irrigated production fields," *Agron. J.*, vol. 95, pp. 1105–1120, 2003.

[27] W. Wiebold *et al.*, "The basics of cleaning yield monitor data," 2003, *North Central Soybean Research Program* [Online]. Available: http://www.planthealth.info/pdf_docs/yield_data_guide.pdf, assessed on May 19, 2012.

[28] G. C. Simbahan, A. Dobermann, and J. L. Ping, "Screening yield monitor data improves grain yield maps," *Agron. J.*, vol. 96, pp. 1091–1102, 2004.

[29] R. Waters, R. G. Allen, M. Tasumi, R. Trezza, and W. G. M. Bastiaanssen, *SEBAL—Advanced Training and Users Manual, Version 1 (from NASA EOSDIS/Synergy grant from the Raytheon Company, through The Idaho Department of Water Resources, USA)*, Kimberly, ID, USA: University of Idaho, 2002, 98p.

[30] S. Liang, "Narrowband to broadband conversions of land surface albedo I algorithms," *Remote Sens. Environ.*, vol. 76, pp. 213–238, 2000.

[31] W. G. M. Bastiaanssen, "SEBAL-based sensible and latent heat fluxes in the irrigated Gediz Basin, Turkey," *J. Hydrol.*, vol. 229, pp. 87–100, 2000.

[32] R. G. Allen, L. S. Pereira, D. Raes, and M. Smith, *Crop Evapotranspiration—Guidelines for computing crop water requirements—FAO Irrigation and drainage paper 56*, Water Resources, Development and Management Service. Rome, Italy: FAO—Food and Agriculture Organization of the United Nations, 1998 [Online]. Available: http://www.fao.org/docrep/X0490 E/X0490E00.htm, accessed on Sep. 2, 2012.

[33] W. G. M. Bastiaanssen, "Regionalization of surface flux densities and moisture indicators in composite terrain: A remote sensing approach under clear skies in Mediterranean climates," Ph.D. dissertation, Department of Eco-Hydrology, Soil physics and Groundwater Management, CIP Data Koninklijke Bibliotheek, Den Haag, The Netherlands, 1995, p. 273.

[34] W. G. M. Bastiaanssen, M. Menenti, R. A. Feddes, and A. A. M. Holtslag, "A remote sensing surface energy balance algorithm for land (SEBAL). 1. Formulation," *J. Hydrol.*, vol. 212–213, pp. 198–212, 1998.

[35] T. Sharma *et al.*, "Procedures for wheat yield prediction using Landsat MSS and IRS-1 A data," *Int. J. Remote Sens.*, vol. 14, pp. 2509–2518, 1993.

[36] J. H. Kastens *et al.*, "Image masking for crop yield forecasting using AVHRR NDVI time series imagery," *Remote Sens. Environ.*, vol. 99, pp. 341–356, 2005.

[37] A. Li, S. Liang, A. Wang, and J. Qin, "Estimating crop yield from multi-temporal satellite data using multivariate regression and neural network techniques," *Photogramm. Eng. Remote Sens.*, vol. 73, no. 10, pp. 1149–1157, 2007.

[38] D. B. Lobell, G. P. Asner, J. I. Ortiz-Monasterio, and T. L. Benning, "Remote sensing of regional crop production in the Yaqui Valley, Mexico: Estimates and uncertainties," *Agric. Ecosyst. Environ.*, vol. 94, pp. 205–220, 2003.

[39] G. Lyle and B. Ostendorf, "A high resolution broad scale spatial indicator of grain growing profitability for natural resource planning," *Ecol. Indic.*, vol. 11, pp. 209–218, 2011.

[40] S. S. Panda, D. P. Ames, and S. Panigrahi, "Application of vegetation indices for agricultural crop yield prediction using neural network techni-ques," *Remote Sens.*, vol. 2, pp. 673–696, 2010.

[41] M. Zhang, P. Hendley, D. Drost, M. O'Meill, and S. Ustin, "Corn and soybean yield indicators using remotely sensed vegetation index," in *Proc. 4th Int. Precis. Agric. Conf.*, Minneapolis, MN, USA, 1998, pp. 1475–1481.

[42] W. G. M. Bastiaanssen and M. G. Bos, "Irrigation performance indicators based on remotely sensed data: A review of literature," *Irrig. Drain. Syst.*, vol. 13, no. 4, pp. 297–311, 1999.

[43] M. F. McCabe, H. Gao, and E. F. Wood, "An evaluation of AMSR-E derived soil moisture retrievals using ground based, airborne and ancillary data during SMEX 02," *J. Hydrometeorol.*, vol. 6, no. 6, pp. 864–877, 2005.

[44] M. M. Hafeez, Y. Chemin, N. Van De Giesen, and B. A. M. Buman, "Field evapotranspiration estimation in central Luzon, Philippines, using different sensors: LANDSAT 7 $ETM+$, Terra MODIS, and ASTER," in *Proc. Symp. Geospat. Theory Process. Appl.*, Ottawa, Canda, 2002 [Online]. Available: http://citeseerx.ist.psu.edu/viewdoc/download?doi=10.1.1.221.9296&rep=rep1&type=pdf

[45] S. M. Ismail and M. H. Al-Marshadi, "Maximizing productivity and water use efficiency of alfalfa under precise subsurface drip irrigation in arid regions," *Irrig. Drain.*, vol. 62, pp. 57–66, 2013.

[46] S. Orloff, D. Putnam, B. Hanson, and H. Carlson, "Implications of deficit irrigation management of alfalfa," in *Proc. California Alfalfa Forage Symp.*, Visalia, CA, USA: UC Cooperative Extension, University of California, Dec. 12–14, 2005 [Online]. Available: http://alfalfa.ucdavis.edu/+symposium/proceedings/2005/05-25.pdf

[47] D. J. Undersander, "Alfalfa (Medicago sativa L.) growth response to water and temperature," *Irrig. Sci.*, vol. 8, pp. 23–33, 1987.

[48] A. Montazar and M. Mohseni, "Optimizing wheat water productivity as affected by irrigation and fertilizer-nitrogen regimes in an arid environ-ment," *J. Agric. Sci.*, vol. 3, no. 3, pp. 143–158, 2011.

[49] J. Liu, R. J. Williams, A. J. B. Zehnder, and H. Yang, "GEPIC—Modelling wheat yield and crop water productivity with high resolution on a global scale," *Agric. Syst.*, vol. 94, pp. 478–493, 2006.

[50] Ministry of Agriculture, *Agricultural Statistical Year Book*. Riyadh, Kingdom of Saudi Arabia: Ministry of Agriculture, 2009.

[51] M. Zhang, P. Hendley, D. Drost, M. O'Meill, and S. Ustin, "Corn and soybean yield indicators using remotely sensed vegetation index," in *Proc. 4th Int. Precision Agric. Conf.*, P. C. Roberts *et al.*, Eds., Minneapolis, MN, USA: American Society of Agronomy, Jun. 19–22, 1998, pp. 1475–1481 [Online]. Available: http://agis.ucdavis.edu/research/PF98_MN3.pdf.

[52] M. H. Kharrou *et al.*, "Crop water productivity and yield of winter wheat under different irrigation regimes in a semi-arid region," *Agric. Sci.*, vol. 2, no. 3, pp. 273–282, 2011.

[53] M. Karimi and A. Gomrokchi, "Yield and crop water productivity of corn planted in one or two rows and applying furrow or drip tape irrigation systems in Ghazvin Province, Iran," *Irrig. Drain.*, vol. 60, pp. 35–41, 2011.

[54] M. Rafiee and G. Shakarami, "Crop water productivity of corn as affected by every other furrow irrigation and planting density," *World Appl. Sci. J.*, vol. 11, no. 7, pp. 826–829, 2010.

[55] M. Moayeri, H. Siadat, E. Pazira, F. Abbasi, F. Kaveh, and T. Y. Oweis, "Assessment of maize water productivity in southern parts of the Karkheh River Basin, Iran," *World Appl. Sci. J.*, vol. 13, no. 7, pp. 1586–1594, 2011.

[56] F. A. Al-Said, M. Ashfaq, M. Al-Barhi, M. A. Hanjra, and I. A. Khani, "Water productivity of vegetables under modern irrigation methods in Oman," *Irrig. Drain.*, vol. 61, no. 4, pp. 477–489, 2012 [Online]. Available: http://onlinelibrary.wiley.com/doi/10.1002/ird.1644/pdf

[57] J. Owens, *et al.*, "Comparing the water use efficiency of tropical pasture grasses and legumes used in Queensland's mixed farming systems," in *Proc. 14th Agron. Conf. Global Issues—Paddock Action*, M. Unkovich, Ed., Adelaide, South Australia, Sep. 21–25, 2008, [Online]. Available: http://www.regional.org.au/au/asa/2008/concurrent/managing-pastures/5916_owensjs.htm

[58] ICARDA, "Sustainable management of natural resources and improvement of the major production systems in the Arabian Peninsula," Arabian Peninsula Regional Program, Int. Center Agric. Res. Dry Areas (ICARDA), Aleppo, Syria, Final Rep. 2000–2005 ICARDA, 2007, p. 69.

[59] M. V. Lopez and J. L. Arrue, "Growth, yield and water use efficiency of winter barley in response to conservation tillage in a semi-arid region of Spain," *Soil Tillage Res.*, vol. 44, no. 1–2, pp. 35–54, 1997.

[60] S. S. Yau, M. Nimah, and M. Farran, "Early sowing and irrigation to increase barley yields and water use efficiency in Mediterranean conditions," *Agric. Water Manage.*, vol. 98, pp. 1776–1781, 2011.

Virupakshagowda C. Patil was born in Rajankollur village, Karnataka, India on May 12, 1953. He received the B.Sc. and M.Sc. degrees in agronomy, and the Ph.D. degree in agronomy from the University of Agricultural Sciences (UAS), Bangalore, Karnataka, India, in 1973, 1975, and 1980, respectively.

During the academic year 1984–1985, he was a Visiting Scientist with the prestigious Commonwealth Forestry Institute, University of Oxford, Oxford, U.K. Currently, he is serving as Chair Professor with the Precision Agriculture Research Chair, Department of Agricultural Engineering, College of Food and Agriculture Sciences, King Saud University (KSU), Riyadh, Saudi Arabia. Before joining KSU, he worked as Dean of College of Agriculture and Special Officer (Technical) with UAS, Raichur, India, in 2008–2010. He served as Instructor with the Department of Agronomy, UAS, Bangalore, India in 1980–1982, Assistant Professor in 1982–1986; and as Associate Professor with UAS, Dharwad, India in 1986–1994, and Professor in 1994–2008. He has successfully implemented 17 extra-mural research projects. He has organized two international and five national conferences and edited the proceedings of all these conferences. He has so far published 90 research papers in peer-reviewed Journals. He has mentored 24 M.Sc. and 8 Ph.D. students. His research interests include precision agriculture and information and communication technologies for the conservation of natural resources.

Prof. Patil is a Fellow of the Indian Society of Agronomy. He is the Founder President of Indian Society of Agricultural Information Technology (INSAIT). From 2006 to 2008, he served as the President of the Asian Federation for Information Technology in Agriculture (AFITA), Japan. Currently, he is Honorary Board Member of AFITA. He is a Member of International Society of Precision Agriculture, Life Member of Indian Society of Agronomy, Indian Society of Weed Science, Indian Society of Remote Sensing, and Institute for Studies on Agriculture and Rural Development, Dharwad, India.

Khalid A. Al-Gaadi was born in Riyadh city, Saudi Arabia, in 1966. He received the M.S. and Ph.D. degrees in agricultural engineering, power and machinery from Colorado State University, Fort Collins, CO, USA, in 1992 and 1998, respectively.

From 1999 to 2002, he was a General Manager with a limited company in Al-Khobar, Saudi Arabia. Between 2002 and 2003, he has been an Assistant Professor with the Department of Agricultural Engineering, College of Agriculture and Veterinary Medicine, King Saud University, Gassim, Saudi Arabia. From 2003 to 2004, he served as an Assistant Professor with the College of Engineering, Al-Gassim University, Gassim. Since 2005, he has been with the Department of Agricultural Engineering, College of Food and Agriculture Sciences, King Saud University, Riyadh, Saudi Arabia. He has been serving as a Full Professor from 2013 to date. He successfully established the Precision Agriculture Research Chair in King Saud University, Riyadh, Saudi Arabia, in 2009 and has been working as a Chair Director from 2009 to date. He represents Saudi Arabia in the International Society of Precision Agriculture, USA. He has presented research papers in International Conferences in USA, Canada, New Zealand, Czech Republic, Turkey, China, Egypt, and India.

Rangaswamy Madugundu was born in Yemmiganur, India, in 1978. He received the M.Sc. degree in botany from Sri Venkateswara University, Tirupati, India, in 2002, and the Ph.D. degree in environmental science and technology from Jawaharlal Nehru Technological University, Hyderabad, India, in 2009.

Since 2011, he has been working as an Assistant Professor with the Precision Agriculture Research Chair, King Saud University, Riyadh, Saudi Arabia. From 2003 to 2008, he was a Research Fellow with the National Remote Sensing Agency, Hyderabad, India. From 2008 to 2011, he served as a Project Scientist (RS&GIS) for the World Bank sponsored project "Monitoring and Evaluation of Watersheds" with the Antrix Corporation Ltd., Bangalore, India, and also served as a GIS expert for the Integrated Watershed Management Programme (IWMP) at Watershed Development Department, Government of Karnataka, Bangalore, India. His research interests include forest biomass and carbon sequestration, evapotranspiration and water productivity mapping of agricultural fields, and NPP of desert farming systems using Eddy covariance and remotely sensed data.

Dr. R. Madugundu was awarded with the Fellowship from Indian Space Research Organization-Geosphere Biosphere Programme (ISRO-GBP) in 2003.

ElKamil H. M. Tola was born in Sudan on January 1, 1963. He received the B.Sc. degree in agricultural engineering from the University of Khartoum, Sudan, in 1985, the M.Sc. degree in the area of conservation tillage in 1995, and the Ph.D. degree from Hohenheim University, Stuttgart, Germany, in 2002, in the area of zero-tillage technology, through DAAD fellowship.

He is an Agricultural Engineer with a teaching background and research work experience. He undertook a Postdoctoral research study in 2005–2007, funded by the JSPS, at the Crop Production Engineering Laboratory of Hokkaido University, Sapporo, Japan in the areas of Precision Farming and Zero Tillage. He was a Visiting Fellow with the University of South Australia in 2008–2009 and worked on GRDC-funded project on zero-till disc coulter mechanics. He worked as Teaching Assistant with the Department of Agricultural Engineering, Faculty of Engineering, University of Khartoum, in 1990–1995, Lecturer "Instructor" in 1996–2002, Assistant Professor in 2002–2009, and Associate Professor in 2009–2011. Since April 2011, he has been working as an Associate Professor with the Precision Agriculture Research Chair, King Saud University, Riyadh, Saudi Arabia. His research interests include conservation agriculture, precision agriculture, sustainable agriculture, and farm power and machinery systems.

Samy Marey was born in Egypt, in 1966. He received the B.Sc. and M.Sc. degrees in agricultural mechanization from Tanta University, Tanta, Egypt, in 1988 and 1994, respectively, and the Ph.D. degree in agricultural engineering from Mansoura University, Daqahlia, Egypt, in 2004.

From 1990 to 1994, he served as Head of the Farm Machinery Maintenance Department, Agricultural Mechanization Sector, Ministry of Agriculture, Egypt. He also worked as a Research Assistant in 1994–2004 and as a Researcher in 2004–2010 with the Agricultural Research Institute, Agricultural Research Center, Dokki, Egypt. He was a Researcher in 2010–2012 with Precision Agriculture Research Chair (PARC), College of Food and Agriculture Sciences, King Saud University, Riyadh, Saudi Arabia. Since 2013, he has been serving as an Assistant Professor with the National Plan for Science and Technology, King Saud University, Riyadh, Saudi Arabia.

Ali Aldosari was born in Wadi Aldwaser, Saudi Arabia on July 10, 1975. He received the Ph.D. degree in geography from Exeter University, Exeter, U.K., in 2006.

He was appointed as a Faculty Member with Geography Department, King Saud University (KSU), Saudi Arabia since 2006. From 2011 to 2014, he served as Head of the Department. He worked as Consultant to the Vice Rectorate for Educational and Academic Affair, KSU, in 2011–2013 and the Knowledge Exchange and Technology Transfer at KSU in 2007–2009. He is also an Internal Consultant to Precision Agriculture Research Chair, KSU since 2010. He led or participated in several funded research projects: Flood assessment in AlQat area, Saudi Arabia, in 2014, Saudi's Dams Evaluation Project in 2013, GIS web-based application in the control of Screwworm disease in Jizan, Saudi Arabia in 2013, Drainage network project of Riyadh, Saudi Arabia in 2013, and the Atlas of Saudi Post Office in 2012. His research interests include the applications of geospatial techniques in agriculture, habitats, population studies, and environmental modeling.

Dr. Aldosari is a Secretary General of Saudi Geographer Society since 2009. He also a member of Saudi Geographer Society, Association of American Geographers, American Society for Photogrammetry and Remote Sensing, and The Urban and Regional Information Systems Associations.

Chandrashekhar M. Biradar was born in Bijapur, India, in 1976. He received the B.Sc. degree in forestry from the University of Agricultural Sciences, Dharwad, India, in 2008, the M.Sc. degree in tree improvement and genetic engineering from the University of Horticulture and Forestry, Solan, India, in 2002, and the Ph.D. degree in remote sensing and environmental sciences from the Department of Space, Indian Institute of Remote Sensing, and University of Pune, India, in 2005.

From 2005 to 2008, he was a Postdoctoral Fellow with the International Water Management Institute, CGIAR Center, then with the Institute for the Study of Earth, Ocean, and Space (EOS), and with the University of New Hampshire, NH, USA. From 2008 to 2013, he served as a Research Professor, Research Scientist, and Manager with the University of Oklahoma, Norman, USA. Currently, he is a Principal Agro-Ecosystems Scientist who heads the Geoinformatics Unit with the International Centre for Agricultural Research in Dry Areas (ICARDA), Amman, Jordan, one of the 15 CGIAR Consortium Research Centers. He published many research papers which include over 40 peer reviewed, 18 books/chapters, over 90 other publications. His research interest includes developing geospatial mechanism for delivering better interventions and package of practices to reach out to smallholding farmers to improve food security and livelihood in the dry areas of the world.

Dr. Biradar has been recognized with the number of international awards and honors such as the Young Scientist of the Year, Outstanding Young Scientist, Best Team Initiative, Outstanding Team Member, Board Member, Steering Committee Member, and Panel Member of Geoinformatics for Agriculture.

Prasanna H. Gowda was born in 1965. He received the M.S. degree in city and regional planning from Mysore University, Mysore, India, in 1990, and the Ph.D. degree in agricultural engineering from Ohio State University, Columbus, OH, USA, in 1996, and the M.B.A degree in strategic management and entrepreneurship from the University of Minnesota, Minneapolis, MN, USA, in 2004.

He served as Graduate Research Associate with the Department of Food, Agricultural, and Biological Engineering, Ohio State University, in 1992–1996. From 1996 to 1998, he was an Associate Researcher with the GIS Division, Upper Midwest Environmental Science Centre, USGS. Between 1998 and 2005, he was a Senior Research Associate and Adjunct Senior Faculty Member with the Department of Soil, Water and Climate, University of Minnesota, St. Paul, MN, USA. Since 2005, he has been a Research Agricultural Engineer with USDA-ARS Conservation and Production Research Laboratory, Bushland, TX, USA. His research interests include evapotranspiration measurement and mapping with thermal remote sensing, irrigation and groundwater management, and hydrologic modeling.

Dr. Gowda's awards and honors include the Outstanding Senior Scientist Award by the Association of Agricultural Scientists of Indian Origin (AASIO), Outstanding Performance Award for 2010 and 2011 (USDA-ARS), and Administrator's Postdoc Award 2010 (USDA-ARS).